Potential Use of Algerian Metallurgical Slag in the Manufacture of Sanitary Ceramic Bodies and Its Effect on the Physical-Mechanical and Structural Properties

Boulaiche, Khaled; Boudeghdegh, Kamel*[+•]

Laboratory of Applied Energetics and Materials (LAEM), Faculty of Sciences and Technology, Process Engineering Department, MSBY Jijel University, ALGERIA

Roula, Abdelmalek

Laboratory of Interactions Material-Environment (LIME), Faculty of Sciences and Technology, Process Engineering Department, MSBY Jijel University, ALGERIA

Alioui, Hichem

Laboratory of Civil Engineering and Environment (LCEE), Faculty of Sciences and Technology, Civil Engineering Department, MSBY Jijel University, ALGERIA

Mahieddine Hamdi, Oualid

Laboratory of Environment, Water Geomechanics and Structures (LEEGO), Faculty of Civil Engineering, USTHB, ALGERIA

ABSTRACT: *A study of the partial substitution of feldspar by Blast Furnace Slag (BFS) and its effects on the properties of sanitary ceramics, has been carried out. Characterization of rheological behavior, thermal, structural, physical, and mechanical properties of fired sanitary-ware bodies, show that 10wt. % is the optimal value for BFS in the formulation of sanitary ceramic. DRX, SEM, and FT-IR analyses confirmed that the starting crystalline phases (quartz and mullite), with the gradual appearance of anorthite, allow a non-negligible improvement in flexural strength (33 to 38 MPa), and a reduction in water absorption (0.35 to 0.10 %). From DTA/TG data, a little change in weight loss during the firing process (8.83 to 9.66 wt. %), was recorded. The Na-electrolytes with a mass ratio Na_2CO_3/ Na_2SiO_3 = 1.5, and a combined mass percentage (0.375 wt. %), are found to give the optimum values for good quality sanitary ceramic slip.*

KEYWORDS: *BFS; Physical properties; Flexural strength; Sanitary ceramic bodies.*

INTRODUCTION

Sanitary ware is one of the most significant and complicated ceramic systems [1]. Its production is generally based on the preparation of the slip from a mixture of clay-kaolin plastic (kaolin 15-20 wt. % and clay

*** To whom correspondence should be addressed.*
+ E-mail: boudeghdegh_k@univ-jijel.dz
1021-9986/2023/2/461-471 11/$/6.01

30-35 wt. %) and other non-plastics 25 wt. % quartz and 25 wt. % feldspar with a suitable amount of water [2]. However, the manufacturing processes of sanitary ware are more or less the same for ceramic products. In the first time, a clay slip is formed by mixing raw materials and water. The rheology is affected by the composition and properties of raw materials. Besides, several types of electrolytes such as sodium silicate and sodium carbonate are added to improve various rheological properties [3, 4]. Afterwards, the slip is poured into a plaster mold, which will absorb water via capillarity, a solid ceramic body is formed before the molds are removed. Following the casting process completion, the pieces are dried and glazed by spraying to improve physical-chemical resistance. Then, the ceramic wares are fired in a tunnel kiln. Finally, the products are colored according to the desired decoration [5, 6]. Generally, we have as completion principal phases in sanitary ceramic bodies: vitreous phase, mullite and residual quartz. The vitreous phase results from the solid-phase reaction of melting feldspar with amorphous silica at around 1050°C. At the same temperature, the spinel phase transforms to form mullite. The cristobalite and the amorphous silica form the residual quartz [7-11].

Over the last few years and until today, the volume of solid wastes has been significantly increasing. According to worldwide statistics [12]. For this reason, the integration of these wastes as substitution materials in various ceramic formulations to reduce the depletion of raw materials has been the subject of several studies. The most mainly used are red clay [13, 14], fly ashes [15, 16] , solid ceramic wastes [17, 18], glass wastes [19, 20] and blast furnace slag [21, 22].

Blast furnace slag (BFS) is an industrial by-product, generated during the production of steel iron. The annual worldwide production is around 390. 000 million Kg [23]. In the north-east of Algeria in particular, the El-Hadjar Iron Factorie produces over 700 million Kg/year of BFS [24]. Due to its low cost, BFS is considered an important alternative material used in the ceramics industry. Some researchers have proven that the use of BFS as a substitution for feldspar improves the microstructure and physical properties. The partial substitution of feldspar by BFS in triaxial porcelain composition increases the strength contribute to the densification and favours the early glazing [8, 25]. In a similar context, glass-ceramics can be prepared from blast furnace slag with an excellent abrasion resistance [26]. Moreover, the incorporation of BFS in wall tile composition increase firepower by 25% and reduces the typical electricity consumption [27]. The use of BFS in traditional ceramic refractory leads to improving the mechanical strength by over 74% [28]. In such a manner, the substitution of sodium feldspar by 15 wt. % BFS in sanitary-ware bodies composition, reducing the sintering temperature by approximately 60 °C and improves mechanical strength by about 67% [29].

In this study, we have investigated for the first time the potential use of Algerian blast furnace slag as a partial substitute for feldspar from 5 up to 20 wt. % to manufacturing new sanitary ware bodies. The first part of this work aims at controlling the rheological behavior of the slip ceramic using Na-electrolytes. The combination of Na_2SiO_3 and Na_2CO_3 allowed the understanding of the rheological properties during the addition of blast furnace slag. The purpose of the second part is to define the optimum composition for obtaining better physical-mechanical and structural properties of fired ceramics.

EXPERIMENTAL SECTION

Raw materials

In the present study, the reference sample E1 of sanitary ceramic slip (0 wt. % BFS) was prepared by mixing 52 wt. % of clay-kaolin with 23 wt. % feldspar and 25wt. % quartz. The feldspar was gradually replaced by BFS to prepare four samples E2, E3, E4 and E5 with an amount of 5, 10, 15 and 20 wt. % BFS, respectively. The Algerian blast furnace slag comes from El-Hadjar Iron-steel Factory, Algeria. The BFS was repeatedly milled until particles reach a size of less than 150μm. The ball clay (Hycast VC) was supplied from United Kingdom. Kaolin Remblend noted as RMB, was provided by Imerys Minerals Ltd; More precisely, it originates from a large open pit in kaolinized granite near St. Cornwall, UK. In addition, PARKAOLIN, from the UK, was also used in slip preparation. The sodium and potassium feldspar were brought from Çine, Aydin, Turkey. Quartz originates from deposits of Bir el-Ater (Tebessa, Algeria).

The chemical composition of raw materials was determined with the X-ray fluorescence spectrometer Rigaku ZSX Primus IV. The loss of ignition (L.O.I) was estimated by heating samples at 1000°C for 2 hours. Table 1 presents the formulations used to prepare slip ceramics.

Table 1: Formulations (in wt. %) of ceramic compositions E1, E2, E3, E4 and E5.

Raw materials	E1	E2	E3	E4	E5
Clay (Hycast VC)	28	28	28	28	28
PARKAOLIN	12	12	12	12	12
kaolin RMB	12	12	12	12	12
Sodium feldspar	12	9.5	7	4.5	2
Potasium feldspar	11	8.5	6	3.5	1
Quartz	25	25	25	25	25
BF Slag	0	5	10	15	20

Sample Preparation

To prepare the sanitary ceramic slip, the raw materials with a suitable amount of water, were milled in a porcelain jar for 4 hours; then up to 1.8 % residue were collected, using a sieve of 63 µm. The amount and type of electrolytes added to the slip are controlled according to the fluidity and density. Then, the resulting slip was cast into a plaster mould at room temperature. On the one hand from each mixture, test pieces (70 × 20 × 10 mm) were prepared to measure water absorption. On the other, rectangular samples (120 × 20× 20 mm) were prepared to measure both linear shrinkage and flexural strength. Furthermore, the samples were dried at room temperature for 48 hours then at 105°C, for 8 hours. Finally, the green bodies were fired in a tunnel kiln for 21 h at 1230 °C under industrial conditions. The values determined for each test represent the average obtained with eight experiments for the same specimen.

Due to the unsatisfactory rheological results of the BFS incorporated and its effect on slip fluidity, an improvement was sought by combining two types of electrolytes; silicates of sodium (Na_2SiO_3, Purity: 99.9%, grade ACS) and carbonate of sodium (Na_2CO_3, Purity: 99.99 %, Alfa Aesar). Initially, the optimum fluidity value was searched by taking 0.1 wt. % of the electrolyte mixture and then measuring its value by changing the additional electrolytes ratios. Then, small proportions of the ideal mixture of electrolytes were added to deduce the amount required to get the lowest fluidity. The fluidity or flow duration of the slip was determined by a measuring the time taken by the slip to fill a 100 ml Ford cup (opening 2.6 mm).

Methods of characterization

The thermal behaviour of green samples was analyzed by differential thermal analysis and thermal weight (TDA/TG) using (TGA-DSC, Universal V4.5A TA Instruments) equipment for temperatures up to 1300 °C, with a heating rate of 5°C / min, in an atmosphere of air. Alumina powder was used as the reference material.

The fired samples were physically characterized; the apparent density (D_A) was determined by Archimedes' method; the total porosity (P %) was calculated by measuring the true density (D_T) by the densimeter Candlot-Le Chatelier; the total porosity is calculated by Eq.1

$$P\ (\%) = \frac{(D_T - D_A)}{DT} \times 100 \quad (1)$$

The linear shrinkage (LS) values are determined, by calculating the difference between the lines recorded on the test pieces before and after firing. Linear shrinkage is calculated by Eq. (2)

$$LS = \frac{(L_0 - L_1)}{L_0} \times 100 \quad (2)$$

Where L_0 is the length value recorded before sintering (10cm). However, L_1 is the length after sintering.

Water absorption (WA) is measured according to ASTM C373-88. 2006; using the weight difference between the weights of dried samples (m_1). These have been subjected to immersing for 2 hours in boiling water, cooling for 12 hours then wiping the surface with a wet towel (m_2). Water absorption is calculated by Eq. (3) [30].

$$WA\ (\%) = \frac{(m_2 - m_1)}{m_1} \times 100 \quad (3)$$

The flexural strength (fs) of the fired samples was measured by a three-point flexural method using the NETSZH global test machine, the measurements are converted into flexural strength by applying Eq. (4)

$$fs = \frac{3}{2}\frac{F * d}{w * t^2} \quad (4)$$

Table 2: Chemical analysis of the raw materials.

Oxides	Clay Hycast VC	PAR KAOLIN	Kaolin RMB	Sodium feldspar	Potasium feldspar	Quartz	BFS
SiO_2	52	48	48	70.74	69.5	96.35	33
Al_2O_3	31	37	37	17.92	17.3	0.52	6.18
TiO_2	1	0.06	0.05	0.26	0	0.05	0.294
CaO	0,2	0.07	0.07	0.5	0.5	1.19	44.1
MgO	0.4	0.3	0.3	0.2	0.2	0.08	3.7
K_2O	2.1	1.9	1.75	0.4	9	0.17	0.681
Na_2O	0.2	0.1	0.1	9.6	3.5	0.08	0.196
Fe_2O_3	1.2	0.19	0.85	0.08	0.16	0.24	1.43
SO_3	0	0	0	0	0	0	1.38
MnO	0	0	0	0	0	0	2
SrO	0	0	0	0	0	0	0.28
BaO	0	0	0	0	0	0	1.01
L. O. I	12	11.8	12.1	0.5	0.4	1.29	0.83

Where F is the failure load (N); d is the distance between two supports; b is sample width and t is sample thickness.

The phases present in the fired ceramics were identified using X-Ray Diffractometer (XRD) with the Advance Bruker D8 diffractometer utilizing Cukα radiation (λ=1.5406 Å). X-ray patterns were registered in the 2θ range from 10 to 100°.

To get more detailed information about the morphology and microstructural characteristics, the microstructure of the fired samples was analyzed by Scanning Electron Microscopy (SEM). The SEM is performed by (WD S, JEOL JSM 6360LV). The micrographs were obtained at 10 kV with a working distance of 11.0 mm, the representative images of the backscattered electrons were taken at a magnifications of 750x.

The infrared transmission spectra were used to investigate the effect on chemical bonds after BFS addition to the composition of sanitary ceramics, the FT-IR curves were extracted using the same weight of sample powder burnt into KBr pellets (purity: 99.9%, Spectral quality). The data are recorded by a spectrophotometer (Shimadzu Japan) in the range 4000-500 cm^{-1}.

RESULTS AND DISCUSSIONS

Chemical analysis

The chemical analysis of the raw materials is given in Table 2. The composition of each batch is summarized in Table 3.

The effect of BFS on rheological parameters of slip

The incorporation of blast furnace slag increased the slip viscosity and slowed its rheological behaviour. Moreover, the addition of electrolytes was needed to improve the rheological behaviour of the slip. Accordingly, the mixing of sodium silicate and sodium carbonate has been conducted. The effect of electrolytes ratio on the fluidity of various slips, is given in Fig. 1. The results, clearly, show that the optimum fluidity is registered at the ratio Na_2CO_3/ Na_2SiO_3=1.5. Fig. 2, shows the effect of the amount of ideal electrolytes mixture on the fluidity of various slips; it can be observed that the fluidity is reduced with the added quantity of the electrolytes mixture, by up to 0.375 wt. %. These results can be related to the excessive amount of sodium cations Na^+ in the medium, which reduces the thickness of the diffusion layer [3]. Some other properties of slip are tabulated in Table 4. It can be noted that the density and pH goes up with the decrease in residue on the sieve induced by BFS additions. The viscosity of the slip greatly affects the surface charge of the ceramic particles, which leads to a change in the pH of slip [31]. In the same context, the use of multiple electrolytes has proven more effective in improving the properties of the slip than the use of sodium silicate only; a similar observation was also made by many authors [32].

Effect of BFS on bulk density, total porosity, firing shrinkage and water absorption of fired samples

The results of bulk density and total porosity measurements for ceramic samples, are presented in Fig. 3.

Table 3: Chemical analysis of slip modified by BFS.

Oxides	E1	E2	E3	E4	E5
SiO_2	70.21	68.45	66.69	64.94	63.18
Al_2O_3	27.18	23.59	23.04	22.49	21.93
TiO2	0.26	0.38	0.39	0.4	0.41
CaO	0.55	2.81	5.12	7.44	9.75
MgO	0.27	0.46	0.64	0.83	1.02
K_2O	2.24	2.04	1.84	1.65	1.45
Na_2O	1.77	1.45	1.13	0.82	0.5
Fe_2O_3	0.61	0.68	0.75	0.82	0.89
SO_3	0	0.07	0.14	0.21	0.29
MnO	0	0.1	0.21	0.31	0.42
SrO	0	0.01	0.02	0.04	0.05
BaO	0	0.01	0.1	0.16	0.21

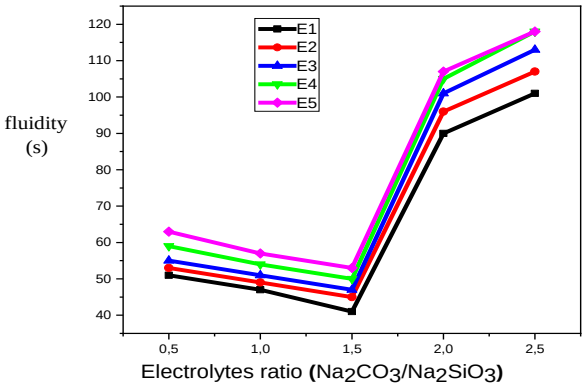

Fig. 1: Variation of the fluidity for different mixtures depending on the ratio between electrolytes (Na_2CO_3 / Na_2SiO_3).

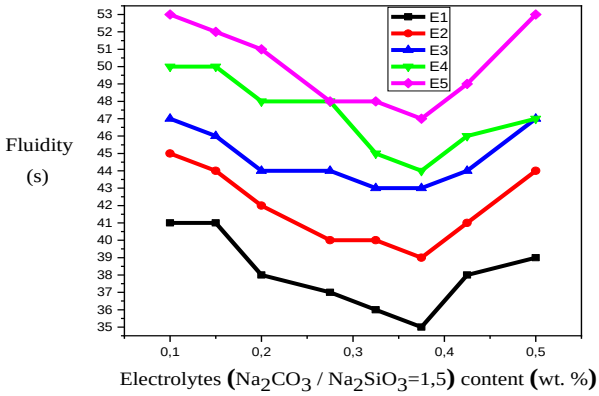

Fig. 2: Variation of the fluidity for different mixtures depending on the content of electrolytes (Na_2CO_3 / Na_2SiO_3 = 1.5).

The density increases with the addition of 10 wt. % BFS, while the porosity decreases; that is mostly due to the formation of the liquid phase resulting from the combination of alkaline earth oxides (CaO + MgO) present in BFS, with alkali oxides (Na_2O + K_2O) present in feldspar. The liquid enhances the sintering reaction and closes the gap between the crystalline phases. Porosity increase may be due to the reduced alkali content in the samples containing BFS [21, 33, 34]. The percentage of water absorption and shrinkage are presented in Fig. 4. Mostly, the decrease in shrinkage is due to the reduction of the liquid phase causing more opening of the pores, which leads to higher water absorption of the samples containing BFS. According to (ASTM C: 326-82) the final shrinkage should usually be smaller than 12%; this enhances the properties of the final products. In addition, According to (ASTM C 373-88), low water absorption (<0.5%) is necessary to ensure hygiene throughout the lifetime of the product [30, 35, 36].

Effect of BFS on flexural strength of fired samples

The influence of BFS on the flexural strength of ceramic samples, is illustrated in Fig.5; a significant increase in flexural strength of ceramic bodies was observed

Table 4: Evolution of the density, residue on sieve and pH of slip as a function of added BFS concentration.

	E1	E2	E3	E4	E5
Density (g/cm^3)	1.771	1.802	1.807	1.817	1.822
Residue on sieve (63 µm) (%)	1.6	1.2	0.9	0.9	0.7
pH	8.3	9.5	10.2	10.4	10.5

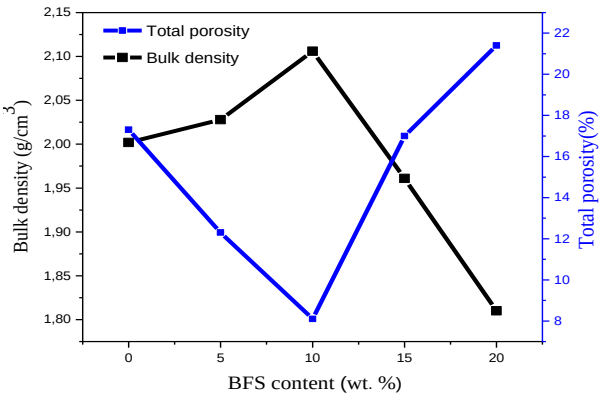

Fig. 3: Variation of water absorption and firing shrinkage for a ceramic heated at 1230°C.

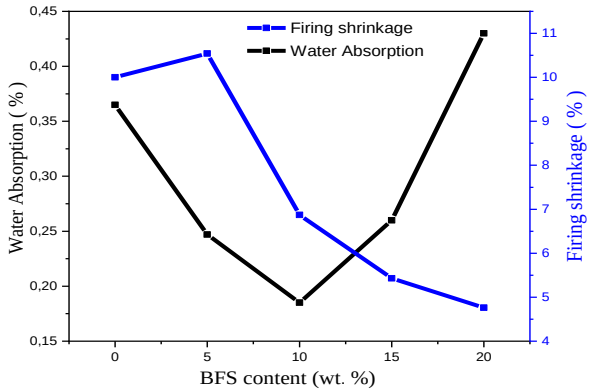

Fig. 4: Variation of water absorption and firing shrinkage for a ceramic heated at 1230°C.

in the case of 10wt. % BFS addition in the ceramic formulation. This flexural strength increase in E3 bodies (41MPa) compared to standard ceramics (33 MPa), can be explained by a higher pre-stress caused by the difference in thermal expansion coefficients between the glass matrix, the formed anorthite grains and the other crystalline phases (quartz and mullite) during the cooling process. The same observations were reported by many authors in previous studies [8, 25].

X-ray diffraction analysis

X-ray diffraction analysis of the fired samples at 1230°C, is shown in Fig.6. E1 the reference sample shows major XRD peaks corresponding to quartz and mullite. While quartz peak remains as it is, mullite peak is decreased by BFS additions (E2, E3, E4 and E5). Anorthite and quartz are the main phases in the E5 containing 20 wt.% BFS. The anorthite formation is due to the high percentage of calcium oxide present in the BFS. The increase of anorthite phase in samples E4 and E5 could be the reason for the decrease in density and flexural strength of fired samples, caused by the lower theoretical density of anorthite phase ~2.7g/cm^3 compared to mullite phase ~3.2g/cm^3 [21, 37, 38].

Microstructure characterization

The physical and mechanical properties observed in ceramic samples are frequently related to microstructural changes during the firing process. SEM micrographs of samples E1, E3 and E5 fired at 1230 °C, are shown in Fig.7. Reference sample E1 appears as glazed and presents a bulk with various particles of different sizes and shapes mostly quartz, some particles of mullite and dissolved feldspar-penetrated clay. Besides, we have the presence of a certain amount of porosity on the surface of crystals [39, 40]. In sample E3, the increase in the melting of BFS leads to the formation of anorthite grain crystals, appearing clearly with quartz grains. The presence of alkaline earth oxides combined with the dissolved earth oxides, allows the formation of an early glass phase leading to the clogging of the pores and increases in the densification of the fired samples. In samples E5, the anorthite phase covers the entire surface with few scattered quartz grains; these results are consistent with the XRD analysis [41].

Thermal analysis

From DTA curves in Fig. 8, we can see that major endothermic peaks appear at ~470 °C, which can be attributed to the dehydroxylation of the hydroxyl groups

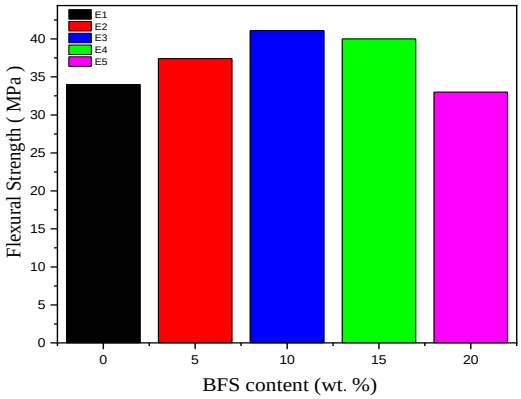

Fig. 5: Evolution of the flexural strength in the case of a ceramic heated at 1230°C.

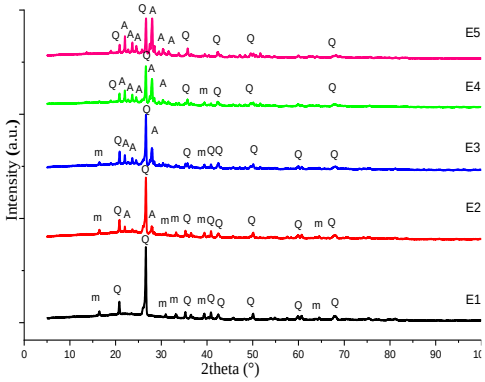

Fig. 6: XRD patterns for heated samples at 1230 °C. (m: mullite,Q: quartz, A: anorthite).

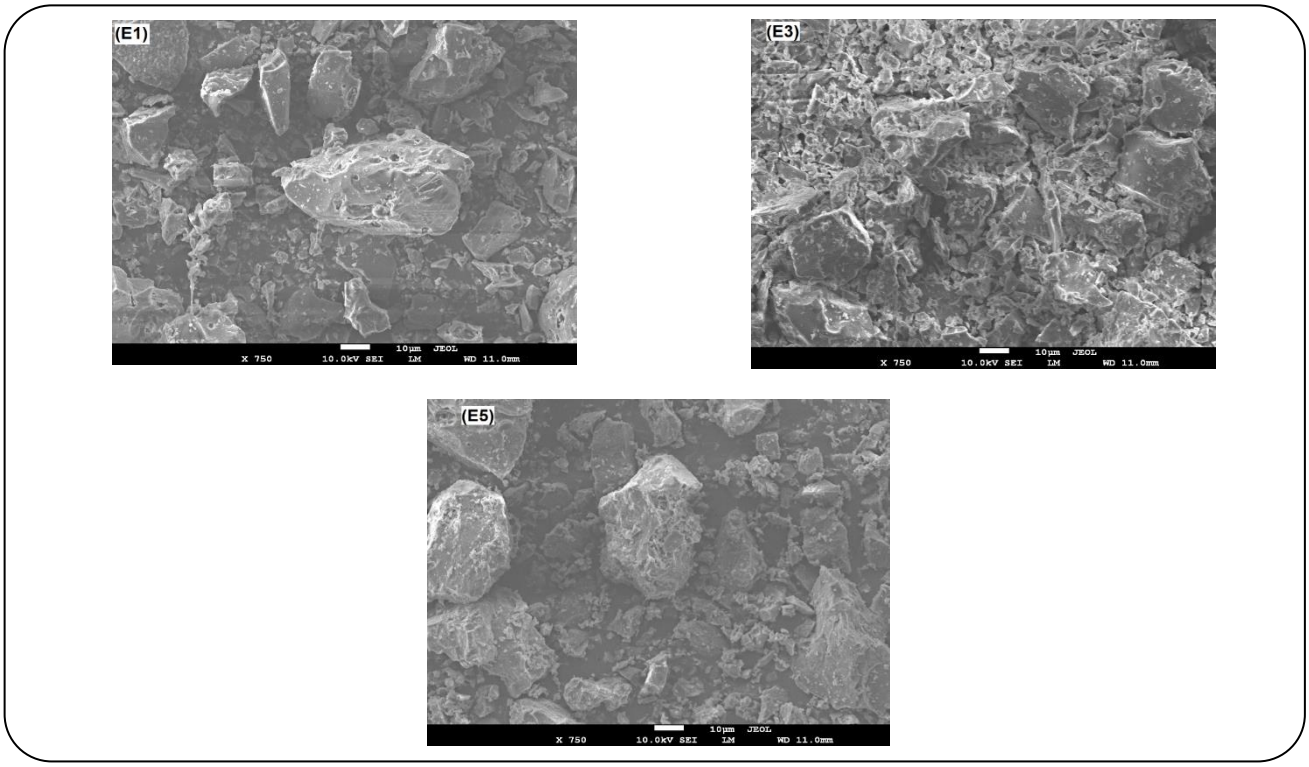

Fig. 7: SEM micrographs of the ceramics E1, E3, and E5.

In kaolin to form metakaolin ($A1_2O_3.2SiO_2$) and also of montmorillonite [8, 11, 42]. Then, we have exothermic peaks at ~970 °C, which are mostly attributed to the transformation of metakaolin into mullite crystals [8, 43, 44]. These microstructural changes are accompanied by a mass loss, as indicated by the curves TGA in Fig.9. The total mass loss values in the mixtures 0, 5, 10, 15 and 20 wt. % BFS, are: 8.83, 9.31, 9.66, 10.06 and 10.18%, respectively. Clearly, BFS has no significant effect on the thermal behaviour of our sanitary ceramic.

FT-IR spectroscopy

Fig. 10 represents the FT-IR spectra of the prepared mixtures. The Si-O bending vibrations observed at 673cm^{-1} in all samples, indicates the existence of quartz and affirms its stability after calcination of the clay,

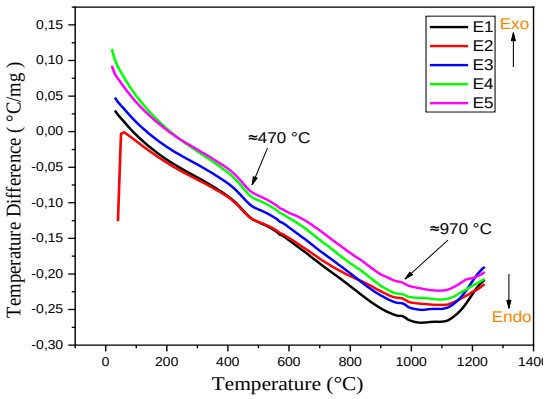

Fig. 8: TDA analysis of the mixtures E1.E2.E3.E4 and E5.

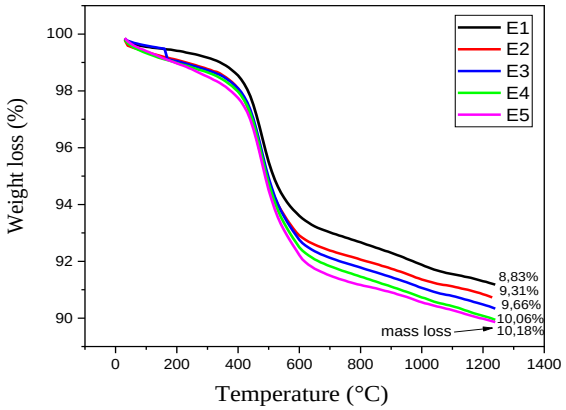

Fig. 9: TGA analysis of the mixtures E1.E2.E3.E4 and E5.

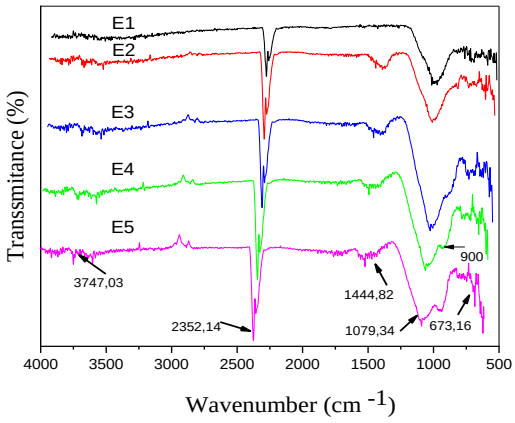

Fig. 10: FT-IR spectra of the ceramics E1.E2.E3.E4 and E5.

this band can be also formed by the stretching mode of Al-O vibration in octahedral coordination [45, 46]. Absorption bands at 900 cm^{-1} identified in samples containing slag, are related to the asymmetric stretching of the AlO_4 groups existing in the glass phases [47, 48]. The bands located at 1079 cm^{-1} can be attributed to Si-O vibrations and (Si-O-Si) asymmetric stretching vibration of siloxane bonds [49, 50] . Wavenumbers at 1444 cm^{-1} are assigned to Si–O–Ca bands, indicating the formation of the anorthite phase from CaO oxide in samples containing BFS; it can also be attributed to the formation of calcite [51, 52]. The bands at 2352 cm^{-1} are due to Si-C stretching [50]. The other peaks situated at 3747 cm^{-1} are assigned to the OH stretching vibrations arising from the Si-OH groups and confirming the transformation of kaolinite into metakaolinite [45, 48].

CONCLUSIONS

Based on the results of this study, BFS waste from the El Hadjar Iron-steel production facility, Algeria, can be used as partial substitute of feldspar in sanitary ceramic body preparation. Indeed, the use of Na-electrolytes in the optimum ratio Na_2CO_3/ Na_2SiO_3=1.5 and a combined amount of 0.375wt. % is found to improve the rheological behaviour of the slip containing BFS. Furthermore, 10 wt. % BFS addition, enhances the flexural strength, densification and reduces water absorption of fired ceramics. According to DRX, SEM and FT-IR analysis, the use of BFS increases anorthite formation. However, there is no significant effect on DTA/TG peaks in the case of kaolinite dehydroxylation and mullite crystallization. The characterization phase, thermal analysis and microstructural evolution support the findings of physico-mechanical properties. These results open new horizons for the use of blast furnace slag in the formulation of sanitary ceramic bodies with many environmental, economical and technical benefits.

Acknowledgments

The authors acknowledge the LEAM laboratory of Jijel University and sanitary ceramic company of El-Milia-Algeria to provide the necessary facilities.

Received : Jan. 16, 2022 ; Accepted : May 16, 2022

REFERENCES

[1] Bomeni I.Y., Wouatong A.S.L., Ngapgue F., Kabeyene K.V., Fagel N., Mineralogical Transformation and Microstructure of the Alluvials Clays, *Science of Sintering*, **51**: 57-70 (2019).

[2] Bernasconi A., Marinoni N., Pavese A., Francescon F., Young K., Feldspar and Firing Cycle Effects on the Evolution of Sanitary-Ware Vitreous Body, *Ceramics International*, **40**: 6389–6398 (2014).

[3] Evcin A., Investigation of the Effects of Different Deflocculants on the Viscosity of Slips, *Scientific Research and Essays*, **6**: 2302-2305 (2011).

[4] Hammadi L., Improving of the Mechanical and Rheological Properties of Slip of Ceramic, *Construction and Building Materials*, **173**: 118-123 (2018).

[5] Silvestri L., Forcina A., Silvestri C., Ioppolo G., Life Cycle Assessment of Sanitaryware Production: A Case Study in Italy. *Journal of Cleaner Production*, **251**: 119708 (2020).

[6] Boudeghdegh K., Diella V., Bernasconi A., Roula A., Amirouche Y., Composition Effects on the Whiteness and Physical-Mechanical Properties of Traditional Sanitary-Ware Glaze, *Journal of the European Ceramic Society*, **35**: 3735-3741 (2015).

[7] Martín-Márquez J., Rincón J., Romero M., Effect of Firing Temperature on Sintering of Porcelain Stoneware Tiles, *Ceramics International*, **34**: 1867-1873 (2008).

[8] Pal M., Das S., Gupta S., Das S.K., Thermal Analysis and Vitrification Behavior of Slag Containing Porcelain Stoneware Body, *Journal of Thermal Analysis and Calorimetry*, **124**: 1169-1177 (2016).

[9] Zanelli C., Raimondo M., Guarini G., Dondi M., The vitreous Phase of Porcelain Stoneware: Composition, Evolution During Sintering and Physical Properties, *Journal of Non-Crystalline Solids*, **357**: 3251-3260 (2011).

[10] Igo A.V., Determination of the Crystallization Temperature of Mullite by Luminescence Spectra of Europium and Chromium Ions, *Physics of the Solid State*, **61**: 2434-2437 (2019).

[11] Boussak H., Chemani H., Serier A., Characterization of Porcelain Tableware Formulation Containing Bentonite Clay, *International Journal of Physical Sciences*, **10**: 38-45 (2015).

[12] Escalante-Garcia J.I., Overview of Potential of Urban Waste Glass as a Cementitious Material in Alternative Chemically Activated Binders, (2015). 10.14062/j.issn.0454-5648.2015.10.14

[13] Sglavo V.M., Maurina S., Conci A., Salviati A., Carturan G., Cocco G., Bauxite 'Red Mud'in the Ceramic Industry. Part 2: Production of Clay-Based Ceramics, *Journal of the European Ceramic Society*, **20**: 245-252 (2000).

[14] Zong Y.-b., Chen W.-h., Liu Y.-x., Xu X.-x., LIU Z.-b., Cang D.-q., Influence of Slag Particle Size on Performance of Ceramic Bricks Containing Red Clay and Steel-Making Slag, *Journal of the Ceramic Society of Japan*, **127**: 105-110 (2019).

[15] Zimmer A., Bergmann C., Fly Ash of Mineral Coal as Ceramic Tiles Raw Material, *Waste Management*, **27**: 59-68 (2007).

[16] Olgun A., Erdogan Y., Ayhan Y., Zeybek B. Development of Ceramic Tiles from Coal Fly Ash and Tincal ore Waste, *Ceramics International*, **31**: 153-158 (2005).

[17] Azevedo A.R.G., Vieira C.M.F., Ferreira W.M., Faria K.C.P., Pedroti L.G., Mendes B.C., Potential Use of Ceramic Waste as Precursor in the Geopolymerization Reaction for the Production of Ceramic Roof Tiles, *Journal of Building Engineering*, **29**: 101156 (2020).

[18] El-Fadaly E., Characterization of Porcelain Stoneware Tiles Based on Solid Ceramic Wastes, *International Journal of Science and Research (IJSR) ISSN*, 2319-7064 (2013).

[19] Gol F., Yilmaz A., Kacar E., Simsek S., Sarıtas Z.G., Ture C., et al. Reuse of Glass Waste In The Manufacture of Ceramic Tableware Glazes, *Ceramics International*, **47**: 21061-21068 (2021).

[20] Marinoni N., D'Alessio D., Diella V., Pavese A., Francescon F., Effects of Soda–Lime–Silica Waste Glass on Mullite Formation Kinetics and Micro-Structures Development in Vitreous Ceramics, *Journal of Environmental Management*, **124**: 100-107 (2013).

[21] Dana K., Dey J., Das S.K., Synergistic Effect Of Fly Ash and Blast Furnace Slag on the Mechanical Strength of Traditional Porcelain Tiles, *Ceramics International*, **31**: 147-152 (2005).

[22] Rahou J., Rezqi H., El Ouahabi M., Fagel N., Characterization of Moroccan Steel Slag Waste: The Potential Green Resource for Ceramic Production, *Construction and Building Materials*, **314**: 125663 (2022).

[23] Rakhimova N.R., Recent Advances in Blended Alkali-Activated Cements: A Review, *European Journal of Environmental and Civil Engineering*, 1-23 (2020).

[24] Alioui H., Chiker T., Saidat F., Lamara M., Aggoun S., Hamdi O.M., Investigation of the Effect of Commercial Limestone on Alkali-Activated Blends Based on Algerian Slag-Glass Powder, *European Journal of Environmental and Civil Engineering*, 1-24 (2021).

[25] Dana K., Das S.K., Partial Substitution of Feldspar by BF Slag in Triaxial Porcelain: Phase and Microstructural Evolution, *Journal of the European Ceramic Society*, **24**: 3833-3839 (2004).

[26] Ma J., Shi Y., Zhang H., Ouyang S., Deng L., Chen H., et al. Crystallization of $CaO–MgO–Al_2O_3–SiO_2$ Glass Ceramic Derived from Blast Furnace Slag *via* One-Step Method, *Materials Chemistry and Physics*, **261**: 124213 (2021).

[27] Ozturk Z.B., Gultekin E.E. Preparation of Ceramic Wall Tiling Derived from Blast Furnace Slag, *Ceramics International*, **41**: 12020-12026 (2015).

[28] Lopez-Perales J., Contreras J.E., Vazquez-Rodríguez F., Gómez-Rodríguez C., Diaz-Tato L., Banda-Muñoz F., et al. Partial replacement of a Traditional Raw Material by Blast Furnace Slag in Developing a Sustainable Conventional Refractory Castable of Improved Physical-Mechanical Properties, *Journal of Cleaner Production*, **306**: 127266 (2021).

[29] Aydin T., Casin E., Mixed Alkali and Mixed Alkaline-Earth Effect in Ceramic Sanitaryware Bodies Incorporated with Blast Furnace Slag, *Waste and Biomass Valorization*, **12**: 2685-2702 (2021).

[30] ASTM C., "Standard Test Method for Water Absorption, Bulk Density, Apparent Porosity, and Apparent Specific Gravity of Fired Whiteware Products". West Conshohocken, Pennsylvania, US: ASTM International. C373-88. (2006).

[31] El-Fadaly E.A., Askar A.S., Aly M.H., Ibrahim D.M., "Rheological, Physico-Mechanical and Microstructural Properties of Porous Mullite Ceramic Based On Environmental Wastes", Boletín de la Sociedad Española de Cerámica y Vidrio, (2020).

[32] Eygi M.S., Ateşok G., An Investigation on Utilization of Poly-Electrolytes as Dispersant for Kaolin Slurry and its Slip Casting Properties, *Ceramics International*, **34**: 1903-1908 (2008).

[33] Ozdemir I., Yilmaz S., Processing of Unglazed Ceramic Tiles From Blast Furnace Slag, *Journal of Materials Processing Technology*, **183**: 13-17 (2007).

[34] Zhao L., Li Y., Zhou Y., Cang D., Preparation of Novel Ceramics With High CaO Content from Steel Slag, *Materials & Design*, **64**: 608-613 (2014).

[35] ASTM, A. C326—Test Method for Drying and Firing Shrinkage of Ceramic Whiteware Clays, In: American Society for Testing and Materials, (1997).

[36] Martini E., Fortuna D., Fortuna A., Rubino G., Tagliaferri V., Sanitser, an Innovative Sanitary Ware Body, Formulated with Waste Glass and Recycled Materials, *Cerâmica*, **63**: 542-548 (2017).

[37] Ismail M., Nakai Z., Sōmiya S. Microstructure and Mechanical Properties of Mullite Prepared by the Sol-Gel Method, *Journal of the American Ceramic Society*, **70**: C-7-C-8 (1987).

[38] Kurama S., Ozel E., The Influence of Different CaO Source in the Production of Anorthite Ceramics, *Ceramics International*, **35**: 827-830 (2009).

[39] Carbajal L., Rubio-Marcos F., Bengochea M., Fernandez J., Properties Related Phase Evolution in Porcelain Ceramics, *Journal of the European Ceramic Society*, **27**: 4065-4069 (2007).

[40] Romero M., Perez J.M., Relación Entre La Microestructura Y Las Propiedades Tecnológicas En Gres Porcelánico. Revisión Bibliográfica, *Materiales de Construcción*, **65**: e065 (2015).

[41] Iqbal Y., Lee W., Microstructural Evolution in Triaxial Porcelain, *Journal of the American Ceramic Society*, **83**: 3121-3127 (2004).

[42] Celik H., Technological Characterization and Industrial Application of Two Turkish Clays for the Ceramic Industry, *Applied Clay Science*, **50**: 245-254 (2010).

[43] Martín-Márquez J., Rincón J.M., Romero M., Effect of Firing Temperature on Sintering of Porcelain Stoneware Tiles, *Ceramics International*, **34**: 1867-1673 (2008).

[44] Roy J., Maitra S., Non-Isothermal Dehydration Kinetics of Diphasic Mullite Precursor Gel, *Iranian Journal of Chemistry and Chemical Engineering (IJCCE)*, **38(4)**: 91-100 (2019).

[45] Adeniyi F.I., Ogundiran M.B., Synthesis of Geopolymer Binders and Mortars from Ijero-Ekiti Calcined Clay, Blast Furnace Slag and River Sand, *Earthline Journal of Chemical Sciences*, **4**: 15-34 (2020).

[46] Roy J., Bandyopadhyay N., Das S., Maitra S., Studies on the Formation of Mullite from Diphasic Al_2O_3-SiO_2 Gel by Fourier Transform Infrared Spectroscopy, *Iranian Journal of Chemistry and Chemical Engineering (IJCCE)*, **30**: 65-71 (2011).

[47] Ismail I., Bernal S.A., Provis J.L., San Nicolas R., Hamdan S., van Deventer J.S., Modification of Phase Evolution in Alkali-Activated Blast Furnace Slag by the Incorporation of Fly Ash, *Cement and Concrete Composites*, **45**: 125-135 (2014).

[48] Gören R., Ersoy B., Özgür C., Alp T., Colloidal Stability–Slip Casting Behavior Relationship in Slurry of Mullite Synthesized by the USP Method, *Ceramics International*, **38**: 679-685 (2012).

[49] Nilforoushan M.R., Otroj S., Talebian N., The Study of Ion Adsorption by Amorphous Blast Furnace Slag, *Iranian Journal of Chemistry and Chemical Engineering (IJCCE)*, **34(1)**: 57-64 (2015).

[50] Joni I.M., Nulhakim L., Vanitha M., Panatarani C., Characteristics of Crystalline Silica (SiO_2) Particles Prepared by Simple Solution Method Using Sodium Silicate (Na_2SiO_3) Precursor, *Journal of Physics: Conference Series*, **1080**: 012006 (2018).

[51] Raizada P., Shandilya P., Singh P., Thakur P., Solar Light-Facilitated Oxytetracycline Removal from the Aqueous Phase Utilizing a H_2O_2/$ZnWO_4$/CaO Catalytic System, *Journal of Taibah University for Science*, 11 (2016).

[52] Ghadami Jadval Ghadam A., Idrees M., Characterization of $CaCO_3$ Nanoparticles Synthesized by Reverse Microemulsion Technique in Different Concentrations of Surfactants, *Iranian Journal of Chemistry and Chemical Engineering (IJCCE)*, **32(3)**: 27-35 (2013).